Reactive Multiphase Flow in Porous Media at the Darcy Scale: a Benchmark proposal

S. de Hoop, D. Voskov, E. Ahusborde, B. Amaziane, M. Kern

May 2021

1 Introduction and context of the proposal

This document presents a proposal for a benchmark on reactive multiphase flow. The proposal was put together as a followup of the first SITRAM meeting `https://sitram19.sciencesconf.org/`, which took place in Pau in December 2019. The topic is increasingly important for modern energy applications.

The content of the benchmark was initially written by SdH and DV, and the current verion is the result of discussions between the five authors. The proposal is still work in progress. Preliminary results will be reported by seveal teams in two sessions of a minisymposium at the upcoming SIAM Conference on Mathematical and Computational Issues in the Gesociences, and it is the organizers' hope that input form the participants will enable the model to be extended towards more realistic geometries as well as physical and chemical phenomena.

A second workshop SITRAM21 will be organized at the end of the year in Paris, where more participants can present results. A special issue of the journal "Computational Geosciences" is planned, where particpants can present and compare their work.

The proposal was written to address several challenges commonly met in applications:

1. Robust coupling of chemical reactions with multiphase flow in porous media,
2. Phase behaviour coupling with equilibrium reactions,
3. Conservative treatment of solid phase dissolution and precipitation,
4. Effective coupling of equations in the case of multiple (concurrent) reactions.

The general structure of the physical and chemical model is described in Sections 2 to 5, while the specific data for the proposed cases are given in Section 6.

2 Governing equations

This section briefly covers the governing equations of the multiphase multi-component reactive transport framework for the proposed benchmark study. We start with the basic mass balance equations including the effect of chemical reactions as source/sink term following [Kala and Voskov, 2020]:

$$\frac{\partial n_c}{\partial t} + l_c + q_c = \sum_{k=1}^{K} v_{ck} r_k^K + \sum_{q=1}^{Q} v_{cq} r_q^Q, \quad c = 1, \ldots, C, \tag{1}$$

where C is a number of species, n_c is the overall mass of component, l_c is the total flux associated with that component, q_c is the total well flow rate associated with that component, v_{ck} is the stoichiometric coefficient associated with kinetic reaction k for the component c and v_{cq} is the stoichiometric coefficient associated with equilibrium reaction q for component c, r_k^K is the rate for kinetic reaction and r_q^Q is the equilibrium reaction rate.

The overall mass of components is defined as

$$n_c = \phi \sum_{j=1}^{P} (\rho_j s_j x_{cj}) + \sum_{l=1}^{M} (1-\phi)\rho_l x_{cl}, \quad c = 1, \ldots, C. \tag{2}$$

Here P stands for the total number of fluid phases and M stands for total number of mineral (solid) phases. Here the first term indicates total mass of component c in all the fluid phases whereas the second term is the mass of component c in the solid phases. The term l_c defines the flux of component c and is given as:

$$l_c = \nabla \cdot \sum_{j=1}^{P} \left(\rho_j x_{cj} \mathbf{u}_j - \rho_j \phi s_j d_{cj} \nabla x_{cj}\right), \quad c = 1, \ldots, C, \tag{3}$$

where the term d_{cj} corresponds to the dispersion of component c in phase j. The term $\mathbf{u_j}$ is the velocity of the phase j and is defined by Darcy's law:

$$\mathbf{u_j} = -\mathbf{K}\frac{k_{rj}}{\mu_j}(\nabla p - \rho_j g \nabla h) \quad j = 1, \ldots, P. \tag{4}$$

Equation 1 can be written in a vector form:

$$\frac{\partial \mathbf{n}}{\partial t} + \mathbf{l} + \mathbf{q} = \mathbf{V^Q r^Q} + \mathbf{V^K r^K}, \tag{5}$$

where $\mathbf{n} = (n_1,\ldots,n_C)^{\mathrm{T}}$, $\mathbf{l} = (l_1,\ldots,l_C)^{\mathrm{T}}$, $\mathbf{q} = (q_1,\ldots,q_C)^{\mathrm{T}}$ is the well flow rate, $\mathbf{V^Q}$ and $\mathbf{V^K}$ are the stoichiometric matrix respectively for the equilibrium and kinetic reactions while $\mathbf{r^Q} = (r_1^Q,\ldots,r_Q^Q)^{\mathrm{T}}$ and $\mathbf{r^K} = (r_1^K,\ldots,r_K^K)^{\mathrm{T}}$ are the equilibrium and kinetic reaction rate vectors.

3 Phase behavior of compositional system

The following equations are used for thermodynamic equilibrium of multicomponent system. A component is in thermodynamic equilibrium if the chemical potential of the components in both phases are equal:

$$f_{c1} - f_{cj} = 0, \quad c = 1, \ldots, C, \quad j = 2, \ldots, P. \tag{6}$$

The fugacity of a component in a particular phase is given by

$$f_{cj} = \phi_{cj} x_{cj} p, \quad c = 1, \ldots, C, \quad j = 1, \ldots, P, \tag{7}$$

where ϕ_{cj} is the fugacity coefficient of an ideal mixture. Equation 6 can also be written in terms of the partition coefficients $K_{cj} = \phi_{cj}/\phi_{c1}$:

$$K_{cj} x_{c,1} - x_{cj} = 0, \quad c = 1, \ldots, C, \quad j = 2, \ldots, P. \tag{8}$$

The system of equations (6) or (8) can be directly coupled with conservation equations (5) and solved in a fully coupled manner using the global Newton solver. Such formulation is often called global or natural formulation. However, when a new phase appears in the process of simulation, the phase equilibrium should be calculated based on the local approximation of the mass from equation (5).

The system of equations can be closed with the following algebraic constraints:

$$\sum_{p=1}^{P} s_p = 1, \tag{9}$$

and

$$\sum_{c=1}^{C} x_{cj} = 1, \ j = 1 \ldots, P \tag{10}$$

In case of equilibrium reactions, we need to add the law of mass action to either global or local systems (depends on the preferred nonlinear formulation) which is given as:

$$Q_q - K_q = \Pi_{c=1}^{C} a_{cw}^{v_{cq}} - K_q = 0, \quad q = 1, \ldots, Q. \tag{11}$$

Here Q is the number of equilibrium reactions, Q_q is the reaction quotient whereas K_q is the equilibrium reaction quotient or equilibrium solubility limit in case of dissolution/precipitation of minerals, a_{cw} is the activity of the component c in the aqueous phase, and v_{cq} is the reaction stoichiometric coefficient.

4 Porosity treatment

For an accurate treatment of solid phase dissolution and precipitation at the continuous level, the treatment of the rock porosity should be adjusted. Conventionally the control volume (denoted as bulk volume) is subdivided into two regions, void space (occupied by all mobile phases, such as liquid and vapor phase) and solid skeleton (occupied by immobile species, for example, carbonate rock).

In most contributions from the literature, the porosity ϕ depends on the concentrations of the minerals according to the relationship:

$$\phi = 1 - \sum_{m=1}^{M} \frac{\mathcal{M}_m c_{ms}}{\rho_m}, \tag{12}$$

where M is the number of reactive minerals, $\mathcal{M}_m$ is the molar mass of mineral m, ρ_m is the mass density of mineral m and c_{ms} represents and the molar concentration of mineral m.

In the equation (12), it is not clear which properties are spatially correlated and which are changing in time due to dissolution or precipitation reactions. Following the approach suggested in [Farshidi, 2016], we can subdivide the volume of the solid skeleton further into a reactive part which can be modified by chemical reactions and a non-reactive part (which is unaltered by any chemical reaction, and therefore constant throughout the simulation), see Figure 1.

Mathematically this is expressed as follows

$$V_b = V_f + V_r + V_{nr}, \tag{13}$$

and V_r denotes reactive volume and V_{nr} represents the non-reactive volume (not altered by any chemical reaction). Dividing this by the total (bulk) volume gives

$$1 = \phi + \phi_r + \phi_{nr} = \phi^T + \phi_{nr}, \tag{14}$$

where ϕ_r represents the reactive volume fraction, ϕ_{nr} is the non-reactive volume fraction, and ϕ^T is the total porosity defined as the sum of the fluid porosity and reactive volume fraction. Since only the reactive volume and fluid porosity can change due to chemical reactions, it follows directly that the total porosity

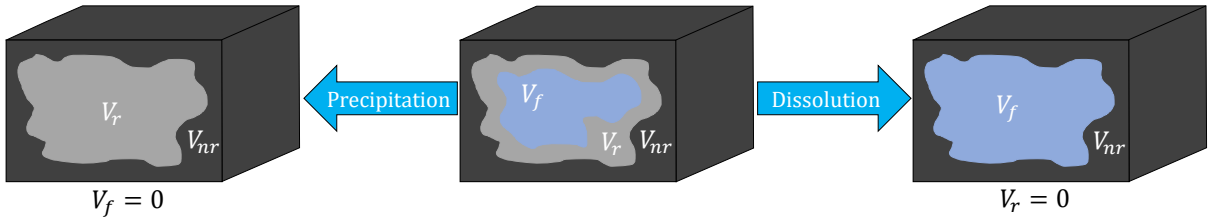

Figure 1: Schematic of the different volumes in the domain. The domain consists of three distinct regions, particularly the fluid volume which is occupies by all the mobile phases (liquid and gaseous in the case of two phase flow), the reactive volume which consist of solid phases that can react or precipitate, and finally the nonreactive volume (the part of the control volume which doesn't participate in any chemical reaction).

remains constant throughout simulation (when neglecting compressibility). This and the changes in volume fractions due to precipitation and dissolution is illustrated in Figure 1.

Note that the fluid porosity can always be obtained with the following constitutive equation

$$\phi = \phi^T \Big(1 - \sum_{m=1}^{M} \hat{s}_m\Big), \tag{15}$$

where M is the number of solid phases (occupying the reactive volume fraction) and $\hat{s}_m$ is the saturation of solid phase. Please note that the s_α is the fluid saturation (defined over the pore volume) while $\hat{s}_m$ is the solid saturation of mineral phase m (defined over the pore and reactive rock volume).

Solid saturation in the total porosity formulation can be found with the following equation

$$\hat{s}_m = \frac{V_{r,m}}{V_r + V_f}, \tag{16}$$

where $V_{r,m}$ is the volume of mineral phase m defined as

$$V_{r,m} = \frac{\mathcal{M}_m}{\rho_m} n_m^r, \tag{17}$$

where n_m^r is the total number of moles of mineral m that can participate in any reaction. This means that in the total porosity formulation, the molar concentration of mineral m is defined as

$$\hat{c}_m = \frac{n_m^r}{V_r + V_f}. \tag{18}$$

and since

$$c_{ms} = \frac{n_m^r + n_m^{nr}}{V_b} = \frac{n_m^r}{V_f + V_r}\frac{V_f + V_r}{V_b} + \frac{n_m^{nr}}{V_b} = \hat{c}_m \phi^T + \frac{n_m^{nr}}{V_b}, \tag{19}$$

where n_m^{nr} is the total number of moles of mineral m that cannot participate in any reaction.

The permeability dependence on porosity is approximated using the following power-law equation

$$k = k_0 \Big(\frac{\phi}{\phi_0}\Big)^A. \tag{20}$$

where k_0 and ϕ_0 are initial porosity and permeability respectively.

5 Additional description for fluid and rock parameters

The relative permeability functions used in this benchmark consist of the Brooks-Corey description, more precisely

$$k_{r,\alpha} = k^e_{r,\alpha}\Big(\frac{s_\alpha - s_{r,\alpha}}{1 - \sum_{p\in P} s_{r,p}}\Big)^{n_\alpha}, \tag{21}$$

where $k_{r,\alpha}$ is the relative permeability, $k^e_{r,\alpha}$ is the maximum relative permeability, $s_{r,\alpha}$ is the residual saturation, and n_α is the Corey exponent of phase α respectively. In the absence of any residual saturation and $P = \{w, g\}$ (i.e., liquid (water) and vapor (gas) phase present as fluid phases in the system), this results in

$$k_{rw} = k^e_{rw}(s_w)^{n_w}, \tag{22}$$

for the water and

$$k_{rg} = k^e_{rg}(1 - s_w)^{n_g}, \tag{23}$$

for the gas relative permeability.

For the phase density, a simple linear compressibility is assumed, particularly

$$\rho_\alpha = \rho_{\alpha,0}(1 + C_\alpha(p - p_0)). \tag{24}$$

Here C_α is compressibility and $\rho_{\alpha,0}$ is density at pressure p_0. This is assumed to hold for each of the three phases present in the system, water, gas, and solid. Additional physical complexity can be obtained by adopting a fully compressible model for the gas phase.

We neglect the effect of capillary pressure in this benchmark, hence eq. (3) contains a single pressure.

Table 1 describes how each component distributes over all phases.

Component	Liquid (water)	Vapor (gas)	Solid
H_2O	✓	✓	✗
CO_2	✓	✓	✗
Ca^{+2}	✓	✗	✗
CO_3^{-2}	✓	✗	✗
$CaCO_3$	✗	✗	✓

Table 1: Component-Phase distribution matrix.

Finally, the activity of each component in the water phase can be written using the following equation

$$a_{cw} = \gamma_{cw} m_{cw}, \tag{25}$$

where γ_{cw} is the activity coefficient and m_{cw} is the molality of component c in the water phase, which in turn can be written as

$$m_{cw} = M_w(\frac{x_{cw}}{x_{ww}}), \tag{26}$$

where M_w is the moles of H_2O per kilogram of aqueous phase (typically taken as 55.508), x_{cw} is the mole fraction of component c x_{ww} is the mole fraction of H_2O in the aqueous phase respectively. For this benchmark the assumption on an ideal solution is made and hence the activity coefficient is taken as 1.

6 Model setup

The following basic model 1D setup is proposed with injection well (i.e., source term) in the first block and production well in the last block, no flow boundary conditions from left and right (i.e., $\frac{\partial p}{\partial x}|_{x=0}= 0$ and $\frac{\partial p}{\partial x}|_{x=\Delta x N_x}= 0$). These are typical reservoir simulation type of boundary conditions. It is possible to replace the wells and no-flow boundary condition with a Neumann boundary condition at $x = 0$ and a Dirichlet at $x = \Delta x N_x$ (with the values for volumetric rate, injection stream, and pressure as found in Table 3).

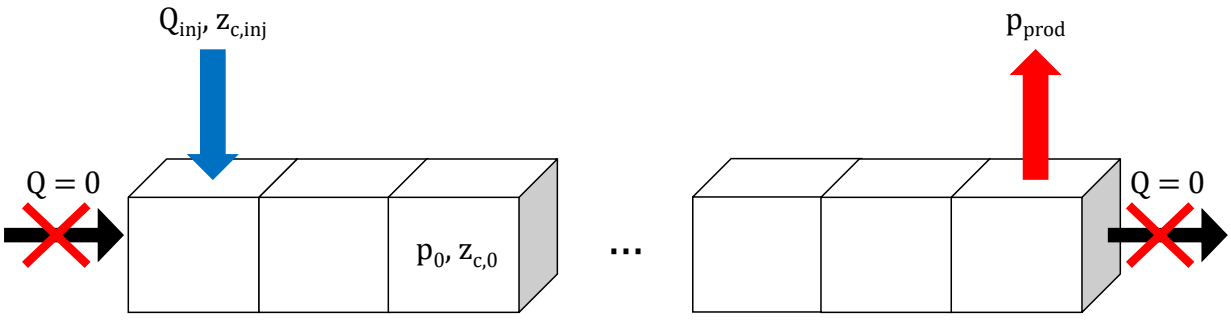

Figure 2: One dimensional domain setup. Injection on the left is constrained with rate and composition Q_{inj} and $z_{c,inj}$ respectively. Production on the right is constrained with pressure p_{prod}. Initial condition for pressure and composition is defined as p_0 and $z_{c,0}$ respectively. No flow boundary condition is imposed on both the left and right boundary.

The rock and fluid related parameters are shown in the Table 2.

Property	Value	Units
Permeability, $k_{x,y,z}$	[100, 100, 100]	[mD]
Total porosity, ϕ^T	1	[-]
Control volume dimension, $\Delta x, y, z$	[1, 1, 1]	[m]
Number of control volumes, N_x	1000	[-]
Phase density at p_0, $\rho_{w,g,s}$	[1000, 100, 2000]	[kg/m^3]
Phase compressibility, $C_{w,g,s}$	[1e-6, 1e-4, 1e-7]	[1/bar]
Phase viscosity, $\mu_{w,g}$	[1, 0.1]	[cP]
End-point relative permeability, $k^e_{rw,rg}$	[1, 1]	[-]
Corey exponents, $n_{w,g}$	[2, 2]	[-]
Residual saturation, $s_{rw,rg}$	[0, 0]	[-]
Phase partition coefficients, K_{H_2O,CO_2}	[0.1, 10]	[-]
Diffusion coefficients, $d_{cj} = d$	1e-9	[m^2/s]
Activity coefficients, $\gamma_{cw} = \gamma$	1	[-]
Porosity-permeability dependence factor, A	3	[-]

Table 2: Values for all the relevant fluid and rock properties.

6.1 Two-phase flow with kinetic chemistry

The first test case consists of a two-phase flow problem with a single kinetic chemical reaction (i.e., we cannot reduce the global system of nonlinear equation using the element reduction). The system consists of the following components: $z_c = [\ \mathrm{H_2O},\ \mathrm{CO_2},\ \mathrm{Ca}^{+2},\ \mathrm{CO_3}^{-2},\ \mathrm{CaCO_3}\ ]$. The kinetic reaction equation consists of

$$\mathrm{CaCO_3} \rightleftharpoons \mathrm{Ca}^{+2} + \mathrm{CO_3}^{-2} \tag{27}$$

The kinetic rate (i.e., the right-hand-side of equation 5) is written as

$$r_k = AK_k \left(1 - \frac{Q}{K_{sp}}\right) \tag{28}$$

where A is the reactive surface area which is a linear function of the solid saturation ($A = A_0\hat{s}_s = (1-\phi_0)\hat{s}_s$), K_k is the kinetic reaction constant, Q is the activity product (to simplify $Q = x_{ca,w} \times x_{co3,w}$) and K_{sp} is the equilibrium constant.

The following Table 3 summarizes the initial, injection and production conditions, simulation time, and kinetic constant.

Property	Value	Units
Injection rate, Q_{inj}	0.2	[m^3/day]
Injection composition, $z_{c,inj}$, $c = 1, \ldots, C-1$,	[0, 1, 0, 0]	[-]
Initial pressure, P_{ini}	95	[bar]
Initial composition, $z_{c,ini}$, $c = 1, \ldots, C-1$,	[0.15, 0, 0.075, 0.075]	[-]
Production pressure, P_{prod}	50	[bar]
Simulation time, T	1000	[days]
Kinetic constant, K_k	1	[-]
Solubility constant, K_{sp}	0.0625	[-]

Table 3: Boundary conditions and other simulation parameters.

Note that composition for the C-th component can be obtained by $z_C = 1 - \sum_{j=1}^{C-1} z_j$ and is not a primary unknown (hence the initial and injection composition doesn't contain the composition of z_C), are primary unknowns in this system are $X = [p, z_1, \ldots, z_{C-1}]$. K_{sp} is equal to $0.25 \times 0.25 = 0.0625$ to ensure that the initial state is in equilibrium and no dissolution occurs.

A Python code will be provided to make it easier to express the boundary conditions in terms of concentrations of individual species for those codes that may need it. Alternatively, the initial and injection composition expressed in terms of molar fraction of individual species and saturation of each phases are given in section 8.

6.2 Two-phase flow with equilibrium chemistry

The second test case is similar to the first one, except that now the reaction is treated as an equilibrium reaction. Mathematically, this adds an additional constraint equation of the form

$$Q - K_{sp} = 0, \tag{29}$$

where Q is the activity product of the equilibrium reaction as defined in equation (11) (which is taken here to have the same form as in Section 6.1) and K_{sp} is the solubility constant, with the value given in Table 3.

All the other parameters, fluid/rock/boundary condition/simulation parameters (as specified in table 2 and 3), are the same as the previous example (including of course the stoichiometry of the reaction).

6.3 3D Heterogeneous domain

The third test case consists of a 3-dimensional heterogeneous domain. Particularly, a zone of high porosity (and permeability), surrounded on the top and bottom with lower porosity (and permeability) zones. The domain extends for 10[m] in the y-direction (all the other measures are mentioned in Figure 3). The boundary conditions are constant injection rate on the left (top half of the domain pure CO2, bottom half pure H2O) and constant pressure on the right boundary (outflow). The test case is executed both with and without gravity (i.e., g=0). Kinetic chemistry is used to model the dissolution of CaCO3. See Table 4 and 5 for all the parameters used in this model. The equations of state for water viscosity and density are changed to reflect the ion concentration (also to more tightly couple the chemistry and two-phase flow). The new equations for water viscosity and density are

$$\rho_w = \rho_{w,0}(1 + C_w(p - p_0) + C_{ions}(X_{w,Ca} + X_{w,CO_3})), \tag{30}$$

where C_{ions} is a constant that reflects the changes of density due to ion-concentration, and

$$\mu_w = \mu_{w,0}(1 + 2C_{ions}(X_{w,Ca} + X_{w,CO_3})). \tag{31}$$

All other parameters (e.g., kinetic constants, reference mass density, etc.) are the same as in test case 6.1.

Property	Value	Units
Gas injection rate, Q_{inj}	1000	[m^3/day]
Water injection rate, Q_{inj}	200	[m^3/day]
Gas injection composition, $z_{c,inj}$, $c = 1, \ldots, C-1$,	[0, 1, 0, 0]	[-]
Water injection composition, $z_{c,inj}$, $c = 1, \ldots, C-1$,	[1, 0, 0, 0]	[-]
Initial pressure on $\Omega_1 \cup \Omega_2$, P_{ini}	95	[bar]
Initial composition on Ω_1, $z_{c,ini}$, $c = 1, \ldots, C-1$,	[0.5, 0, 0.25, 0.25]	[-]
Initial composition on Ω_2, $z_{c,ini}$, $c = 1, \ldots, C-1$,	[0.15, 0, 0.075, 0.075]	[-]
Production pressure, P_{prod}	50	[bar]
Simulation time, T	1000	[days]

Table 4: Boundary conditions and other simulation parameters.

7 Expected output

The expected output for the test-case specified in section 6.1 is shown on Figure 4 hereafter.

8 Appendix

```
Properties based on injection state: state = [P, z_h2o, z_co2, z_ca, z_co3]
Injection state =  [1.65e+02 1.00e-12 1.00e+00 1.00e-12 1.00e-12]
```

Property	Value	Units
Porosity on Ω_1, ϕ	1	[-]
Permeability on Ω_1, $k_{x,y,z}$	[3703, 3703, 3703]	[mD]
Porosity on Ω_2, ϕ	0.3	[-]
Permeability on Ω_2, $k_{x,y,z}$	[100, 100, 100]	[mD]
Total porosity on $\Omega_1 \cup \Omega_2$, ϕ^T	1	[-]
Control volume dimension, $\Delta x, y, z$	[10, 10, 10]	[m]
Number of control volumes, $N_x \times N_y \times N_z$	$124 \times 1 \times 24$	[-]
Diffusion coefficients, $d_{cj} = d$	1e-5	[m^2/s]
Water density and viscosity coefficient, C_{ions}	1	[-]
Gravitational acceleration, g	9.8	[m/s^2]

Table 5: Values for all the relevant fluid and rock properties.

```
-------------------------------------------------------------------------------
                 H2O         CO2         Ca+2        CO3-2       CaCO3
Composition, z_c 1.00e-12    1.00e+00    1.00e-12    1.00e-12    1.00e-12
Liquid MoleFrac  1.00e-11    1.00e-02    4.94e-01    4.94e-01    0.00e+00
Vapor MoleFrac   1.00e-12    1.00e+00    4.94e-13    4.94e-13    0.00e+00
Solid MoleFrac   0.00e+00    0.00e+00    0.00e+00    0.00e+00    1.00e+00
-------------------------------------------------------------------------------

-------------------------------------------------------------------------------
                 Liquid      Vapor       Solid
Phase MoleFrac   1.02e-12    1.00e+00    1.00e-12
Mass Density     1.00e+03    1.01e+02    2.00e+03
Viscosity        1.00e+00    1.00e-01    0.00e+00
Sat. phi_tot     1.17e-13    1.00e+00    1.00e-12
Sat. phi_fluid   1.17e-13    1.00e+00    0.00e+00
-------------------------------------------------------------------------------


Properties based on initial state: state = [P, z_h2o, z_co2, z_ca, z_co3]
Initial state =  [9.5e+01 1.5e-01 1.0e-12 7.5e-02 7.5e-02]
-------------------------------------------------------------------------------
                 H2O         CO2         Ca+2        CO3-2       CaCO3
Composition, z_c 1.50e-01    1.00e-12    7.50e-02    7.50e-02    7.00e-01
Liquid MoleFrac  5.00e-01    3.33e-12    2.50e-01    2.50e-01    0.00e+00
Vapor MoleFrac   5.00e-01    3.33e-12    2.50e-01    2.50e-01    0.00e+00
Solid MoleFrac   0.00e+00    0.00e+00    0.00e+00    0.00e+00    1.00e+00
-------------------------------------------------------------------------------

-------------------------------------------------------------------------------
                 Liquid      Vapor       Solid
```

```
Phase MoleFrac    3.00e-01   0.00e+00   7.00e-01
Mass Density      1.00e+03   1.00e+02   2.00e+03
Viscosity         1.00e+00   1.00e-01   0.00e+00
Sat. phi_tot      3.00e-01   0.00e+00   7.00e-01
Sat. phi_fluid    1.00e+00   0.00e+00   0.00e+00
--------------------------------------------------------------------------------
```

References

[Farshidi, 2016] Farshidi, S. F. (2016). *Compositional reservoir simulation-based reactive-transport formulations, with application to CO2 storage in sandstone and ultramafic formations.* PhD thesis, Stanford University.

[Kala and Voskov, 2020] Kala, K. and Voskov, D. (2020). Element balance formulation in reactive compositional flow and transport with parameterization technique. *Computational Geosciences*, 24(2):609–624.

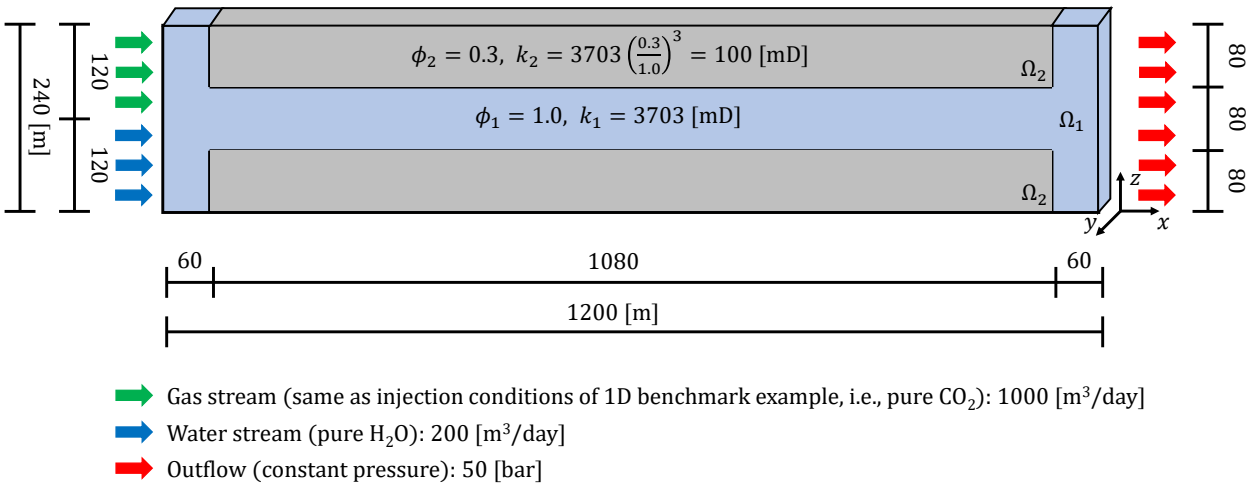

Figure 3: Configuration of the third test case (Chapter 6.3). Constant injection rate on the left boundary (Neumann) and constant pressure (Dirichlet) on the right. The domain extends 10[m] in the y-direction.

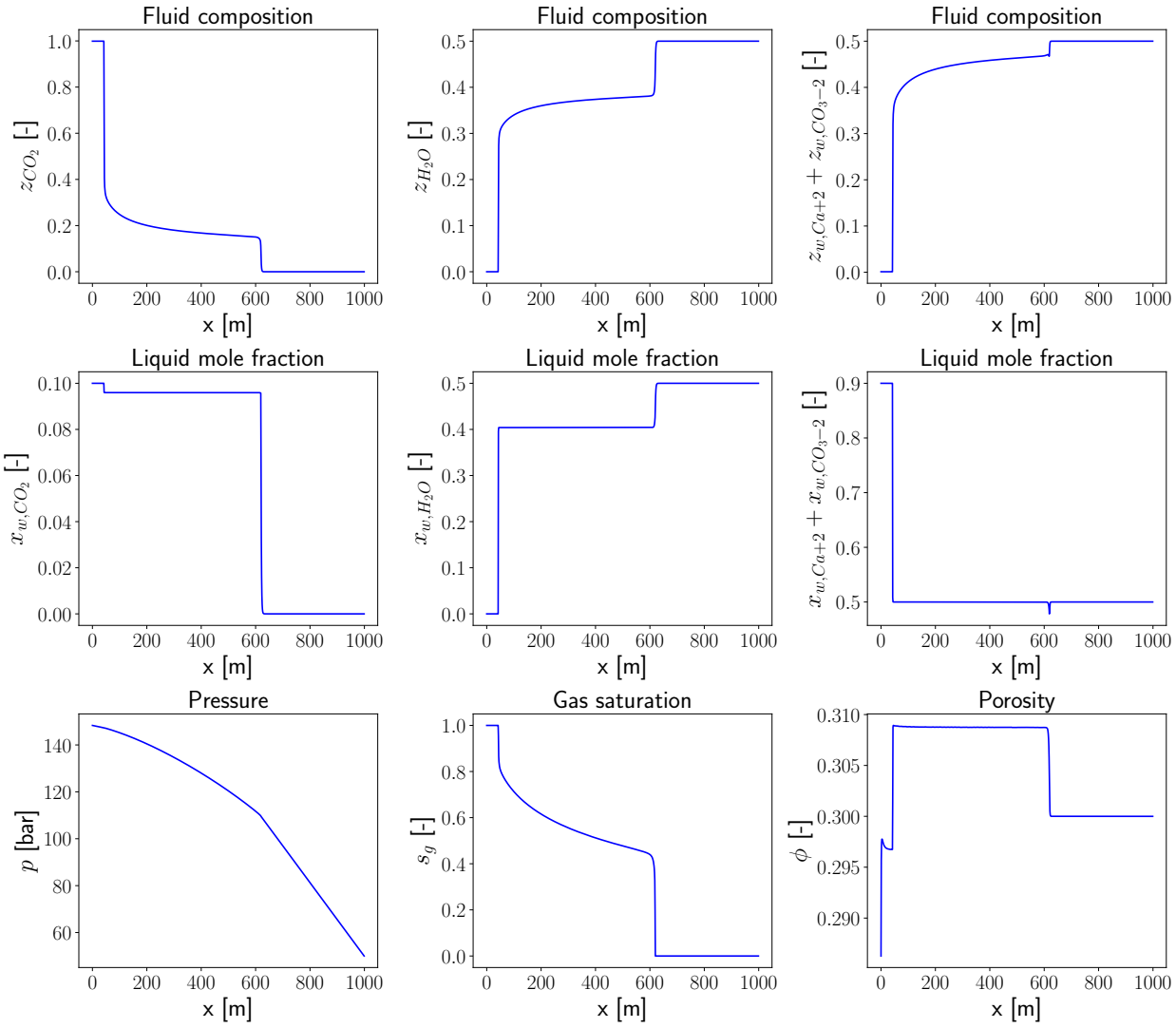

Figure 4: In the initial stage, due to the absence of ions in the injection stream, dissolution of the CaCO3 occurs, since the solution is under-saturated. However, the vaporization of the H2O due to the CO2 injection causes precipitation to occur, hence the porosity reduces close to the injection point (left boundary).